Mask pattern transferred transient grating technique for molecular-dynamics study in solutions

Koichi Okamoto,[a] Zhaoyu Zhang, and Axel Scherer
Department of Electrical Engineering, California Institute of Technology, Pasadena, California 91125

David T. Wei
Wei and Associates, 3715 Malibu Vista Drive, Malibu, California 90265

(Received 28 May 2004; accepted 4 October 2004)

We have developed a mask pattern transferred transient grating (MPT-TG) technique by using metal grating films. Transient thermal grating is generated by an ultraviolet light pattern transfer to nitrobenzene in 2-propanol solution, and the subsequent effect is detected through its diffraction to a probe beam. The thermal diffusion coefficient is obtained by the relationship between the grating periods and the signal decay lifetime, and is well in agreement with the calculated value. This technique has many advantages, such as a simple setting, an easy alignment, accurate phase control, and high stability for molecular-dynamics study in solutions. © *2004 American Institute of Physics*. [DOI: 10.1063/1.1828591]

The transient grating (TG) technique,[1,2] which is one of the third-order nonlinear spectroscopy, has been a powerful tool to monitor several photonics and photochemical processes in solutions since its onset. For a brief history, solutions were photoexcited by an optical interference pattern generated by two crossing pump beams. As parameters, several properties of a solution were spatially modulated according to the interference pattern and were detected through the diffraction of the probe beam. The time varying profiles of the diffracted signal indicate the many processes in solution, such as electron transfer, molecular dynamics, heat dynamics, ultrasonic, volume/structure change, clustering/aggregation, and chemical reaction, etc.[3–8] The optical heterodyne detected-TG (OHD-TG) technique[9–16] had also been developed later to improve the sensitivity. The reference beam, which has the same direction, polarization, and wavelength as the signal beam, was superimposed to the signal beam to amplify the signal intensity. The experimental set ups of the OHD-TG were very difficult, because the probe and reference beams need to be aligned and tuned within submicrometer scale to meet the phase-matching condition. Very recently, Katayama *et al.* developed a lens-free OHD-TG technique[17,18] by using a transmission grating structure in a 3-mm glass. This technique was easier than the traditional OHD-TG technique. In this Letter, we describe a more convenient and easy, well-aligned technique, the mask pattern transferred-TG (MPT-TG) technique, by using a metal film grating fabricated in our laboratory.

Figure 1(a) shows the scanning electron microscope (SEM) image of the smallest metal grating film (400-nm metal width and 1-μm period). Chromium layer (100 nm) was created by the vacuum evaporation on the quartz substrate. A fine grade resist was deposited on a Cr layer by spin coating. Nano- or micrometer-scaled patterns are written by the lithography of an electron beam or a direct writing laser. Finally, metal grating structures are engraved by chemical etching. The principle of the MPT-TG is depicted in Fig. 1(b). A finished metal grating film is suspended into the sample solution and the excitation UV pump beam (I_e) is incident at the grating in solution. Thus, the grating pattern is transferred from the metal film to the sample solution under near-field condition (Fresnel diffraction). This is similar to the traditional photolithography but, in this case, the sample material is a liquid solution. The solute molecules were excited by this special TG structure. A part of the probe beam (I_p) irradiated on the grating in the solution is diffracted under the far-field condition (Fraunhoffer diffraction) and was detected by the photodetector.

The experimental set up of the MGT-TG is schematically shown in Fig. 2. A frequency tripled Nd:YAG laser (λ_e = 366 nm, I_e = 0.3 mJ/pulse) was used as a pump beam. The pulse width and repetition rate are 10 ns and 3 Hz, respectively. A cw-He-Ne laser (λ_p = 633 nm, I_p = 0.05 mW) is used as a probe beam. Both beams are focused by a lens on the sample solution in a quartz cell (10-mm spacing). Diffraction beam is limited and passes through a pinhole and a glass filter, and is registered with an InGaAs photodetector. Two types of signals, diffracted by permanent metal grating (I_r) and transient grating (I_s), are simultaneously detectable. The permanent grating signal plays the role of the reference beam of the OHD-TG set up and amplifies the transient grating signal. Both diffracted signals pass the color filter and pinhole to be separated from the pump beam and detected onto the photodetector.

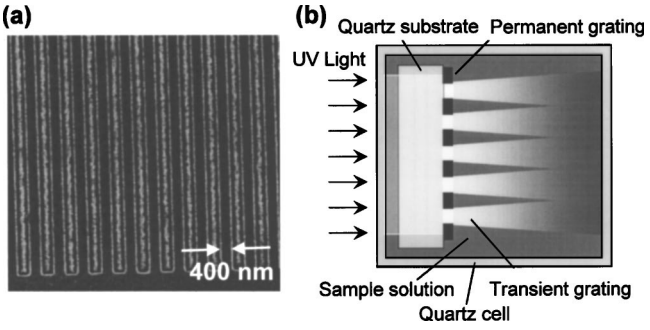

FIG. 1. (a) Scanning electron microscope (SEM) image of the smallest fabricated nanometal grating. (b) Schematic diagram of the pattern transfer from the metal grating film to the solution.

[a]Electronic mail: kokamoto@caltech.edu

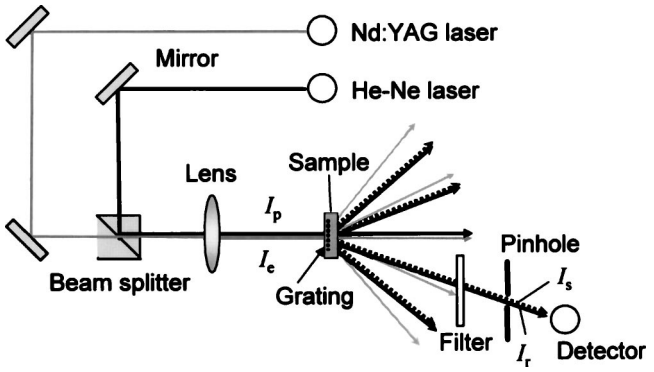

FIG. 2. Experimental set up of the MPT-TG technique with metal grating and the optical configurations of irradiated pump (I_e) and probe (I_p) beams, and diffracted reference (I_r) and signal (I_s) beams.

The sample solution was nitrobenzene in 2-propanol (5 vol %). The excited energy of nitrobenzene is immediately converted to the molecular vibration, translation, and finally, heat energy. Such nonradiative relaxation processes of nitrobenzene are completed within a very short time scale (a few hundred picosecond).[19] Therefore, nitrobenzene has been used often as the standard solution of the typical heat source (molecular heater) for photothermal measurement.

Figure 3 shows the semilog plot of the time-dependent diffraction signals with (a) micrometer-scaled and (b) nanometer-scaled etch width metal grating, respectively. We found the exponential decay component (I_s) superimposed on the large nondecayed offset component (I_r). The former is due to the transient grating, while the latter is due to the permanent grating, respectively. According to the theory, detected total signal intensity (I_{total}) can be described by[17,18]

$$I_{total}(t) = I_r + 2a\left[\chi^{(3)\prime}(t)\cos\Delta\phi + \chi^{(3)\prime\prime}(t)\sin\Delta\phi\right] I_e I_p + \left|\chi^{(3)}(t)\right|^2 I_e^2 I_p, \tag{1}$$

where $\chi^{(3)\prime}(t)$ and $\chi^{(3)\prime\prime}(t)$ are the real and imaginary parts, respectively, of the third-order nonlinear electrical susceptibility $\chi^{(3)}(t)$, and a is a real constant. The third term indicates the TG signal with usual homodyne detection and is negligible because it involves $\chi^{(3)}$ in solution and should be very small. Thus, only the second term of Eq. (1) indicates I_s. In this case, $\chi^{(3)\prime}(t)$ and $\chi^{(3)\prime\prime}(t)$ are equal to the refractive index change $\delta n(t)$ and the absorbance change $\delta k(t)=0$ at 633 nm induced by the transient grating, respectively. $\Delta\phi$ is the phase difference between I_r and I_p. In the OHD-TG techniques, unstable $\Delta\phi$ has been the main difficulty of the experimental set up. However, in our set up, $\Delta\phi$ is decided only by the structure and thickness of the metal grating. Therefore, the phase stability is excellent without the tuning of beam lines in this set up. Thus, $\sin\Delta\phi$ in Eq. (1) should be a constant, and I_s should be proportional to $\delta n(t)$.

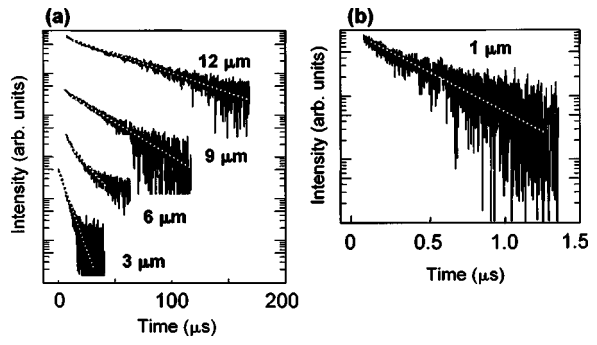

FIG. 3. Time profile of the diffracted signals with metal grating of (a) 12-, 9-, 6-, and 3-μm periods and (b) 1-μm period. The dashed lines were fitted by the exponential functions.

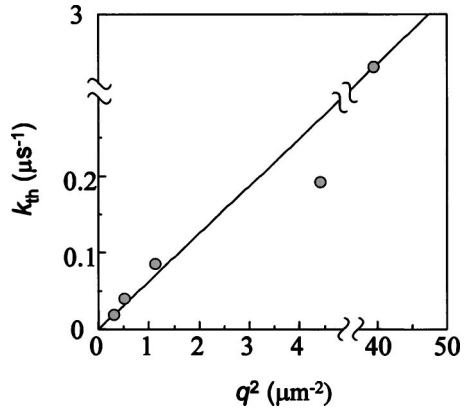

FIG. 4. Relationship between the square of the grating constants (q^2) and the decay rate (k_{th}) of the TG signals. This slope indicates the thermal diffusion coefficient.

The spatial modulation of the optical intensity (δI_e) induced the spatial modulation of the population of the molecular excited states (δP), temperature (δT), and density of solvent ($\delta\rho$). Namely, δn should be attributed to δT and $\delta\rho$ in this time scale. Temperature rising increase $\delta\rho$, which decrease δn. Therefore, the spatial distribution of temperature (thermal grating) was created, and the signal decay shows the thermal diffusion processes in solution. By solving the Fourier's diffusion equation, the time profile of $\delta n(t)$ is given by[20]

$$\delta\hat{n}(t) = \left[\left(\frac{\partial n}{\partial \rho}\right)_T \left(\frac{\partial \rho}{\partial T}\right) + \left(\frac{\partial n}{\partial T}\right)_\rho\right] \frac{Q}{\rho C_p} \delta I_e[C]\exp(-D_{\text{th}} q^2 t), \tag{2}$$

where, Q, C_p, and $[C]$ are the heat energy released from unit molecules, specific heat capacity, and solute molecular concentration, respectively. $\delta\hat{n}(t)$ is the spatial Fourier component of $\delta n(t)$. q is the grating constant described by the grating period (Λ) as $q=2\pi/\Lambda$. D_{th} is the thermal diffusion coefficient of the solution. Therefore, the signal decay rate ($k_{\text{th}}=1/\tau$) obtained by the exponential fitting was described by $k_{\text{th}}=D_{\text{th}}\,q^2$. Figure 4 shows the relationship between k_{th} and q^2 at each grating period, where a good linear relationship and the D_{th} value are shown by the slope. The obtained value ($D_{\text{th}}=7.0\pm0.7\times10^8$ m^2 s^{-1}) is very close to the calculated value ($D_{\text{th}}=6.8\times10^8$ m^2 s^{-1}) (Ref. 18) by the thermal conductivity (k) of 2-propanol as $D_{\text{th}}=\kappa/\rho C_p$. This agreement demonstrates the validity of this method according to the signal analysis above. By the same token, several diffusion processes, such as the molecular diffusion in solution, energy migration in materials, or the carrier diffusion in semiconductors, should be measurable.

The MPT-TG technique should have many merits for photonic and photochemical application. The experimental set up and the beam alignment of the MPT-TG are simpler and easier than those of the usual OHD-TG technique, while it has very high signal sensitivities and signal-to-noise (S/N) ratios for the optical heterodyne detection. The pump and probe beam should be incident at the same spot on the metal

grating film, but the tunings of direction and phase of the beams are not necessary. The lens-free OHD-TG technique[17,18] has similar merits, but the MPT-TG technique has still more merits comparing to the lens-free technique. In the lens-free technique, the optical interference pattern was constructed by the diffraction light with transmission grating on the sample located behind the grating. The phase differential $\Delta\phi$ can be controlled by the distance ($\sim$250 μm usually) between the grating and the sample. In the MPT-TG technique, metal film grating is suspended into the sample solution and the transient grating structure is created directly behind it. Thus, $\Delta\phi$ is decided only by the thickness of the metal layer and the incident angle. Therefore, $\Delta\phi$ stability is controllable by the thickness of the metal layer. Moreover, various patterns can be used flexibly with any metal widths and periods to optimize the sensitivity. The measurement of the grating periods dependence is also very easy by sliding the film to change the pattern structure.

In conclusion, our technique by using nano- or micro-metal grating film has many advantages compared to the traditional techniques. This technique should be a powerful and useful tool for wider applications in physics, chemistry, material, and biological applications.

The authors would like to thank Professor M. Terazima (Kyoto University) for valuable suggestions and discussions. We also thank Dr. T. Yoshie (Caltech) for helping with the nanofabrication. The authors greatly acknowledge support from the DARPA Center for Opto-fluidics, under Grant No. HR0011-04-1-0032.

[1]Y. R. Shen, *The Principle of Nonlinear Optics* (Wiley, New York, 1984).
[2]H. J. Eichler, P. Gunter, and D. W. Pohl, *Laser-Induced Dynamic Grating* (Springer, Berlin, 1986).
[3]M. D. Fayer, Annu. Rev. Phys. Chem. **33**, 63 (1982).
[4]M. Terazima, K. Okamoto, and N. Hirota, J. Phys. Chem. **97** (1993) 13387.
[5]L. Dhar, J. A. Rogers, and K. A. Nelson, Chem. Rev. (Washington, D.C.) **94**, 157 (1994).
[6]J. A. Rogers and K. A. Nelson, J. Appl. Phys. **75**, 1534 (1994).
[7]M. Terazima, Res. Chem. Intermed. **23**, 853 (1997).
[8]M. Terazima, Adv. Photochem. **24**, 255 (1998).
[9]G. D. Goodno, G. Dadusc, and R. J. D. Miller, J. Opt. Soc. Am. B **15**, 1791 (1998).
[10]G. D. Goodno and R. J. D. Miller, J. Phys. Chem. A **103**, 10619 (1999).
[11]M. Terazima, Chem. Phys. Lett. **304**, 343 (1999).
[12]M. Terazima, J. Phys. Chem. A **103**, 7401 (1999).
[13]G. Dadusc, J. P. Ogilvie, P. Schulenberg, U. Marvet, and R. J. D. Miller, Proc. Natl. Acad. Sci. U.S.A. **98**, 6110 (2000).
[14]R. Torre, A. Taschin, and M. Sampoli, Phys. Rev. E **64**, 061504 (2001).
[15]Q.-H. Xu, Y.-Z. Ma, I. V. Stiopkin, and G. R. Fleming, J. Chem. Phys. **116**, 9333 (2002).
[16]N. Gedik, J. Orenstein, R. Liang, D. A. Bonn, and W. N. Hardy, Science **300**, 1410 (2003).
[17]K. Katayama, M. Yamaguchi, and T. Sawada, Appl. Phys. Lett. **82**, 2775 (2003).
[18]K. Katayama, M. Yamaguchi, and T. Sawada, Chem. Phys. Lett. **377**, 589 (2003).
[19]R. W. Yip, D. K. Sharma, R. Giasson, and D. Gravel, J. Chem. Phys. **88**, 5770 (1984).
[20]M. Terazima, K. Okamoto, and N. Hirota, J. Phys. Chem. **97**, 5188 (1993).